6-1-2009

Hydrological Behavior of Grasslands of the Sandhills of Nebraska: Water and Energy Balance Assessment from Measurements, Treatments and Modeling

Venkataramana Sridhar
Boise State University

David A. Wedin
University of Nebraska

Hydrological Behavior of Grasslands of the Sandhills of Nebraska: Water and Energy Balance Assessment from Measurements, Treatments and Modeling

Venkataramana Sridhar
Boise State University

David A. Wedin
University of Nebraska

Abstract

Understanding energy and water balance processes in the Sandhills is crucial to assess the land-atmosphere feedback effects. The Sandhills located in western Nebraska covers a vast grassland ecosystem with limited variability in vegetation and soil. However, the combined effect of topography, land cover and micrometeorology by subjecting the land surface to various disturbances and treatments is rarely studied. The NOAH Land Surface Model was used to estimate net radiation, latent, sensible and ground heat fluxes as well as water balance components for two growing seasons between 2005 and 2006 in various plots at the Grasslands Destabilization Experimental site where these plots were subjected to four different treatments and located at two topographical locations namely high and low positions. The simulated results of net radiation and ground heat fluxes correlated well with measurements. While the amount of precipitation received was between 900 and 1000 mm for both seasons, on a daily and sub-daily time scale, the partitioning of net radiation into latent, sensible and ground heat fluxes showed high variability across the plots, primarily driven by vegetation and soil moisture. Total evapotranspiration and soil moisture averages suggested the influence of vegetation and timing of precipitation also in controlling various land surface processes in the Sandhills. This study provides a framework for using the LSM to quantify the feedback effects and emphasizes the importance of microtopography and land treatments in the model environment.

Introduction

The critical need for understanding land-atmospheric exchanges is well recognized (e.g., Dirmeyer, 1994; Entekhabi et al., 1992; Nicholson, 2000). Numerous successful experimental studies including First ISLSCP Field Experiment (FIFE) (e.g., Murphy, 1992; Kanemesu et al., 1992), SGP97 (e.g., Jackson et al., 1999; Mohanty et al., 2000; Sridhar et al., 2003) as well as numerical modeling studies to quantify the near-surface energy-balance partitioning (e.g., Li and Islam, 2002; Lakshmi and Wood, 1998) and boundary layer processes have been continuously pursued for over two decades and the results of these studies directly contributed to better understanding of the intractable land surface processes including drought and to improved short-term weather forecasting. Despite persistent efforts, the complexity of land surface hydrology demands answers to many questions in order to precisely manage our land and water resources, especially in vulnerable 'spots'. The role of soil moisture in modulating precipitation generation is extremely high in 'transition zones' between wet and dry climates (Koster et al., 2004), as evaporation becomes sensitive to soil moisture in these areas. The Great Plains of the Continental U.S. and in particular, the Sandhills of Nebraska can be characteristically identified with this phenomenon simply due to the fact that evaporation is greater than precipitation during the growing season, thus implying that the region predominantly serves as a source for moisture.

The Sandhills covers a vast grassland ecosystem with mainly two distinct types of vegetation: short and tall grass prairie. In this precipitation-limited semi-arid region, it is assumed that the grasslands play a crucial role in stabilizing the sand dunes and also serve as an important driver in the land-atmospheric exchange process. Sridhar et al., (2006) reported that the combination of westward shift of southerly winds (i.e. southerly winds shifting to westerly) that deprived moisture transport to the region and the diurnal heating of the desiccated land surface contributed to the mega-droughts of the Sandhills in the medieval warm period. Sridhar (2007) showed the

variability of growing season evapotranspiration in the Sandhills using the crop coefficients technique and emphasized the importance of high-resolution physically-based modeling of fluxes over this landscape. Various studies on soil moisture, evapotranspiration and/or groundwater interaction have been reported. For instance, Chen and Hu (2004) on the Sandhills, Webb and Leake (2006) on the riparian watershed in Southern Arizona, Sandvig and Phipps (2006) on the ecohydrology-soil moisture linkages in semiarid regions, have shown the dynamic nature of the subsurface, surface and atmospheric interaction. Kahan et al., (2006) found that Sahelian energy and water balance simulations were greatly influenced by vegetation and soil parameterization including leaf area index, stomatal conductance, thermal diffusivity and hydraulic conductivity. Eberbach (2003) reviewed the hydrology of the native and disturbed ecosystems in southern Australia and showed the vibrancy of ground water recharge regimes in relation to vegetation in these ecosystems. Sandvig and Phillips (2006) reported that vegetation impacts are significant on soil moisture fluxes, climate and vadose zone characteristics in arid to semiarid regions.

Various measures have been initiated recently to characterize both water and energy budgets in the Sandhills with various treatment processes, their resilience to the disturbance introduced in the system, role of vegetation for the stability of dunes and the recharge of ground water beneath the Sandhills. Paucity of surface and atmospheric observations so far limited high-resolution coupled modeling to estimate energy and water budget in the Sandhills. Nevertheless, quantifying soil moisture and evapotranspiration in this dune landscape covered with native grasslands either observationally or through modeling is constantly recognized as critical in order to fully understand and accurately partition both energy and water balance components. Soil moisture beneath the root zone in the Sandhills ecosystem is greatly affected when the vegetation cover is cleared or grazed and can impact the water cycle and water movement as recharge into the groundwater reservoir (Sridhar et al., 2006). Interestingly, the interactions among the surface, subsurface and atmospheric systems are simplified to an extent in this landscape as the entire soil column is sandy and both soil and the grass cover are generally homogeneous over this region. To achieve the ultimate objective of quantifying the potential recharge to the ground water system and to evaluate alternate management practices in order to preserve the ecosystem integrity, it is therefore essential to understand the impact of vegetation and their role in partitioning surface energy and water balance in the Sandhills. There has been no study until now to firmly suggest how the Sandhills' land cover impacts energy and water balance at the plot scale level. In order to understand the entire Sandhills dynamics, it is also of paramount importance to quantify evapotranspiration, soil moisture and the surface energy balance components using high quality spatio-temporal vegetation, weather information and validate the land surface model simulation results with flux measurements collected over the two year period.

The objective of this study is to partition both energy and water balance components in multiple plots at the Grasslands Destabilization Experimental (GDEX) site that are subjected to four different treatments and each at two topographical locations namely high and low elevations for two growing seasons between 2005 and 2006 and validate the NOAH Land Surface simulation with available measurements, including net radiation, ground heat flux and soil moisture. This paper assesses the response of the Sandhills grasslands to the disturbance introduced to the native ecosystem as well as the climate variability from the high and low elevation sites. Additionally, this investigation also addresses the effects of temporal aggregation, their usefulness in analyzing the energy and water balance components at the hourly, daily, monthly and interannual timescales and characterizing the responses of vegetation, soil moisture and precipitation interplay for the two growing seasons. This investigation was carried out with the NOAH Land Surface Model (LSM). This land surface model formulation continues to be part of the MM5/WRF (weather research forecasting) family of models in an off-line mode to simulate water balance and energy fluxes. Using field observations of soil moisture, net radiation and ground heat flux, our study evaluated the simulated energy and water balance components. This study is useful to assess the water budget closure at the plot scale level and therefore can serve as a basis for formulating model drivers in order to accurately quantify the hydrological components over the Sandhills ecosystem.

Study Area: Grasslands Destabilization Experiment

The Grasslands Destabilization Experimental site is located in the east-central region of the Sandhills (Figure 1). The site characteristics are provided in Table 1.This site, shown in Figure 1 is also co-located with the Barta Brothers Ranch, an automated weather data network (AWDN) micrometeorological site, operated by the High Plains Regional Climate Center (HPRCC). The GDEX site has a combination of rolling prairies with upland grasslands (5-15 % slope, total relief <20 m) and interdunal valleys that are predominantly dry, unlike other valleys that are wet between October and April in the Sandhills. The experimental site contains 10 plots, each 120 m x 120

m in upland grasslands. Traditionally these areas were grazed for each growing season for more than 50 years. As this experiment deals with short-term study, the area was subjected to treatments as explained below. The soil is mostly sandy to loamy sand (85-90% sand, soil organic matter 0.7-0.8% to 15cm depth) (i.e., bare sand < 25%) and is abundant with C4 grasses (*Andropogon hallii*, *Calamovilfa longifolia*, *Schizachyrium scoparium*). Other vegetation types include C3 grasses, low woody shrubs (*Amorpha canescens*), forbs and cacti. As stated earlier, the plots are broadly subjected to four different treatments in two different topographic settings categorized as high and low: grazed, control, long-term (press) disturbance, short-term (pulse) disturbance. There is also a bare soil plot at this location which is not considered for any of the simulation and interpretations as part of this investigation. A Surface-Energy balance and Soil Moisture (referred as SESM) instrumentation set up measuring a suite of weather and soil moisture variables, is housed in these plots. The treatments at GDEX included grazed, control, long-term (press) disturbance, and short-term (pulse) disturbance. From Table 1, it is worth noting that the elevation differences between high and low can only be considered as nominal (within 7 m), however, these microtopographical variations may be expected to have a role in the distribution of soil moisture, net radiation as well as exert an influence on the boundary-layer processes. The plots were equipped with instruments for collecting the data on weather variables, soil moisture, soil temperature and surface fluxes continuously.

Grazed plots: The rotational grazing study conducted at the Barta Brothers Ranch site includes these plots and numbered as P9 and P10. Since they are located in different quarter section pastures on an 8-pasture rotational unit, grazing operation for these two plots was never undertaken at the same time. SESM 1/Grazed/Low is located at P9.

Control plots: There are 4 combinations of SESM stations in these treatment plots of P2 and P4. Two stations, SESM 3/Control/High and SESM 7/Control/Low are in P2, and the other two stations, SESM 4/Control/High and SESM 8/Control/Low are in P4. These plots are neither grazed nor treated with herbicide. They are also fenced in order to avoid cattle trespassing and hence any extraneous physical disturbance.

Long-Term (Press) disturbance: Plots P1 and P8 are under this treatment where SESM station configuration and pre-treatment data collection was initiated in May 2004. P1 contains SESM 2/Press Disturbance/High and SESM 6/Press Disturbance/Low. P8 contains SESM 5/Press Disturbance/High and SESM 9/Press Disturbance/Low. The herbicide applied at these plots periodically since 2005 keeps vegetation dead in them and will be maintained in the same condition at least for the next 5 years. This kind of treatment is important in the sandhills to record how and when the sand dunes show signs of destabilization or activation. A cattle fence is constructed around these plots also to avoid any external damages to the actual disturbance.

Short-term (Pulse) disturbance: The disturbance caused to these plots, namely P3 and P6, are periodic but not on a long-term basis. The grass cover was destroyed with herbicide in May 2005 and there was no physical disturbance allowed but remained de-vegetated through 2005. However, there was no herbicide treatment in 2006 and there has been a dramatic growth of annual weeds and this vegetation recovery will continue through 2007. Neither of these two plots has SESM stations and we used the averages of SESM 2/Press Disturbance/High , 3, 4 and 5 for Pulse High and the averages of SESM1/Grazed/Low, 6, 7, 8, and 9 for Pulse Low. That is, precipitation, temperature, wind speed, solar radiation, longwave downwelling radiation and specific humidity were calculated from all High sites for Pulse High and all Low sites to Pulse Low. The variability within micrometeorological drivers within this 1 km^2 area was not significant as compared to topographical positions and vegetation condition and therefore the assumption of averaging weather variables did not impact our model runs or interpretation of results.

Data

SESM data loggers

Since 2004, quality-checked, continuous 30-minute data sets were archived from the SESM stations. At each high and low topographic location in plots 1, 2, 4, 8 and 9, a single SESM station was set up to monitor the environmental conditions. The variables that were measured at 1.5 m above the surface include air temperature, relative humidity, net and solar radiation. Soil moisture and soil temperature below the surface at 10, 25, 50 and 100 cm depths were also simultaneously measured. Two soil heat flux plates at 6 cm below the surface measured ground heat flux continuously. However, the heat storage above 6 cm was not adjusted and its impact on our comparisons was also discussed later. Wind speed data at 1.5 m and precipitation were observed only at five SESM stations 1, 2, 3, 4 and 5. For the other SESMs, we used the average of these five stations in this study.

The SESM stations collected data every 30 minutes. The temperature / humidity sensors are in a passively ventilated shield (from Campbell Scientific 41303-5A 6-Plate Gill Radiation Shield). Other instruments deployed and the measurement technologies employed were as follows: (1) Cup anemometer, rotating magnetic reed switch (Met One Instruments 014A) (2) Platinum resistance thermometer (Vaisala Humitter 50Y) (3) Solid state capacitive moisture sensor (Vaisala Humitter 50Y) (4)Silicon photodiode (LiCor LI-200 0.41 μm – 1.08 μm bandwidth) (5) Silicon photodiode (LiCor LI-200 0.41 μm – 1.08 μm bandwidth) (6) Differential thermopile sensor (Kipp & Zonen NR Lite 0.3 μm – 30 μm bandwidth) (7) Differential thermopile sensor (REBS HFT3) (8) Type E thermocouple (Omega Engineering) (9) AC dielectric constant (Delta-T Devices Theta Probe ML2) (10) Tipping bucket magnetic reed switch (Texas Electronics 525M)

Data were logged on Campbell Scientific CR10X data loggers equipped with AM16/32 electro-mechanical multiplexors. A thermister temperature sensor (Campbell Scientific model 107) was physically attached to the multiplexor body, near the soil thermocouple terminals and served as the reference junction. Power was provided by a 50W solar panel coupled to a 100 Ahr deep cycle marine battery through an automatic charge controller. Battery voltage and internal data logger temperatures were also recorded for diagnostic purposes. All instruments were read once every second, and averages were computed and saved at the end of every half hour. The data recorded were thus half hourly averages consisting of 1800 individual readings. The time stamp associated with each line of data representd the end of the half hour averaging period.

The raw data files were periodically downloaded and the data were archived and quality controlled. The QA/QC procedure was done automatically by a Fortran program. The program examined each data item and (if the instrument was installed) determined if it was between a pre-defined maximum and minimum value for that particular sensor. QC flags were then associated with each datum to summarize the results of these checks. If a sensor was not installed, or was known to be non-functional, the value –9999.0 is inserted for any "noise data" present. The program also applied linear calibration factors (offset and gain) to all sensors. This allowed "matching" of sensor pairs.

Vegetation data

From two large (5 m x 8m) subplots in each plot, vegetation activity was measured non-destructively and the variables measured were leaf area index (LAI) and fraction of Photosynthetically Active Radiation (fPAR). Root biomass and length were also measured monthly. The LAI data was available biweekly throughout the growing season for two years. Four 0.25 square meter quadrats per plot were clipped at ground level every three weeks during the growing season (April 1 - October 30). Samples were sorted while fresh into the categories graminoid (grasses and sedges), forbs, current year growth on shrubs, and dead plant organic matter. The live plant subsamples were analyzed for leaf area using a Licor 3000 leaf area meter. LAI was calculated as the ratio of life plant leaf area to sampled ground area. Our methods to determine the root distribution began prior to imposing experimental treatments in 2004 by collecting four 3-meter deep soil cores with a truck-mounted hydraulic soil corer in each plot. These cores were separated into 20cm horizons, and washed over a 1 mm screen prior to weighing.

In order to calculate latent heat flux, NOAH LSM needs vegetation fraction which is the fraction of green vegetation that covers the ground. This is normally derived from LAI and NDVI measured from satellite or ground-based sensors. In this study, we collected LAI which was used to compute Normalized Difference Vegetation Index (NDVI) using equation (1) developed by Gutman and Ignatov (1998) and applied by Yunhao et al. (2003)

$$NDVI_g = NDVI_\infty - (NDVI_\infty - NDVI_o)\exp(-kLAI) \qquad (1)$$

The extinction coefficient, k, ranges between 0.8 and 1.3 and a value of 1 was assumed (Yunhao et al., 2003). $NDVI_g$ calculated from equation 1 was subsequently used to obtain vegetation fraction interpolated at the daily time step using an algorithm developed by Gutman and Ignatov (1998). The basic assumption is that the vegetation is dense and the equation is given by:

$$\sigma_f = \frac{NDVI_g - NDVI_o}{NDVI_\infty - NDVI_o}$$

(2)

The parameters used in equation (1) are $NDVI_\infty$ of 0.9 and $NDVI_o$ of 0.04 for dense vegetation and bare soil conditions. $NDVI_g$ is the green NDVI corresponding to the observed LAI as in equation (1). σ_f is the green vegetation fraction (dimensionless) and LAI is the leaf area index. The derived vegetation fraction used for the model simulations is shown in Figure 2. This is one of the important parameters used by NOAH LSM in partitioning net radiation into sensible, latent and ground heat fluxes.

NOAH-Land Surface Hydrology Model

Model Description

The land surface hydrology model (LSM) is part of the MM5/WRF family of models and it is widely used operationally and validated in different regions over vast areas at the local, regional, continental and global scales (e.g, Sridhar et al., 2002; Chen and Dudhia, 2001). We used this model in an off-line mode to address the primary question of partitioning of energy and water balance components at the GDEX site by utilizing the densest spatio-temporal forcing and other data collected during the growing seasons of 2005-06. The model was implemented for each of the treatment plot taking advantage of SESM weather measurements and the plot-wise vegetation data. This provided a key opportunity to identify the patterns relating to the partitioning of the fluxes on various low and high topographic and land treatment conditions based on model estimates of the surface energy-balance components. We, however, validated net radiation and ground heat flux estimates with measurements and based our confidence limits implicitly on latent and sensible flux estimates.

The physical processes formulated in the model and the sequences of simulation of each of the energy budget components, including net radiation, latent, sensible and ground heat fluxes and water budget components such as runoff, soil moisture, evaporation has been documented and described elsewhere (Chen and Dudhia, 2001; Sridhar et al., 2002). It is, however, beneficial to state the salient features of the model so that the continuity is enhanced in the narration of this investigation. We implemented the LSM with one canopy layer and four soil layers with a total depth of 2 m below the surface. The layers are configured as 10, 30, 60 and 100 cm thick. While the upper 1 m is designated as root zone layer, the lower 1 m acts as a reservoir with gravity drainage at the bottom. The energy-balance equation at the surface is given by this equation:

$$Rn = LH + SH + G \qquad (3)$$

Once net radiation (R_n) is computed as the difference between incoming and outgoing radiation, it is partitioned into three components as shown in the right hand side of equation *3* as latent heat (*LH*), sensible heat (*SH*) and ground heat (*GH*) fluxes.

Soil Hydrology

The prognostic equation for the volumetric soil water content (θ) in the hydrology model is given by:

$$\frac{\partial \theta}{\partial t} = \frac{\partial}{\partial z}\left(D \frac{\partial \theta}{\partial z} \right) + \frac{\partial K}{\partial z} + F_\theta \qquad (4)$$

where D and K are the soil water diffusivity ($m^2\ s^{-1}$) and hydraulic conductivity ($m\ s^{-1}$), respectively, and both are functions of θ; t and z are time (s) and the vertical distance (m) from the soil surface downward (i.e., the depth), respectively; and F_θ represents sources and sinks (i.e., precipitation, evaporation and runoff). This diffusive form of the relationship is known as Richard's equation and is derived from Darcy's Law for movement of water in soils (with the assumption of a rigid, isotropic, homogeneous, and one dimensional vertical flow domain) (Hanks and Ashcroft, 1986). K and D are highly non-linear functions of soil moisture and in particular when the soil is dry, they can change several orders of magnitude for a small variation in soil moisture. As the soil- related parameterization is very sensitive to the diurnal partitioning of surface energy into latent and sensible heat (Cuenca et al., 1996), Chen

and Dudhia (2001) suggested the investigation of alternative soil hydraulic parameterization schemes that would reflect the relationship between hydraulic conductivity and soil water content.

Surface runoff is addressed in the LSM using the Simple Water Balance (SWB) model approach given by Schaake et al. (1996). The SWB model is a two-reservoir hydrological model that has been well calibrated for large river basins. It takes into account the spatial heterogeneity of rainfall, soil moisture, and runoff. The total evaporation is the sum of the direct evaporation from the top shallow soil layer, evaporation of precipitation intercepted by the canopy, and transpiration through the canopy via water uptake by roots. The bare soil evaporation scheme is governed by soil wilting point and field capacity, green vegetation fraction cover, and a Penman-based energy balance approach for potential evaporation. Evaporation of rainfall intercepted by the canopy is a function of the canopy intercepted water content, which depends upon the total precipitation and the precipitation that reaches the ground. The canopy transpiration is determined by:

$$E_t = \sigma_f E_p B_c \left[1 - \left(\frac{W_c}{S} \right)^n \right] \tag{5}$$

where E_t is canopy transpiration (m s^{-1}), σ_f is the green vegetation fraction (dimensionless), E_p is potential evaporation (m s^{-1}), W_c is the canopy intercepted water content (mm), S is the maximum allowed value for W_c (specified here as 0.5 mm), and n = 0.5 (dimensionless). B_c is a function of canopy resistance and is expressed as:

$$B_c = \frac{1 + \dfrac{\Delta}{R_r}}{1 + R_c C_h + \dfrac{\Delta}{R_r}} \tag{6}$$

where C_h is the surface exchange coefficient for heat and moisture (m s^{-1}), Δ is the slope of the saturation-specific humidity curve (dimensionless), R_r is a function of surface air temperature, surface pressure and C_h (dimensionless), and R_c is the canopy resistance (s m^{-1}). Details on C_h, R_r and Δ are given by Ek and Mahrt (1991) and R_c is discussed by Jacquemin and Noilhan (1990).

Soil Thermodynamics

One of the primary functions of the coupled land surface model is to provide the near-surface layer of an atmospheric model with sensible and latent heat fluxes, and surface skin temperature to compute upward longwave radiation. The surface skin temperature is determined following Mahrt and Ek (1984) by applying a single linearized surface energy balance equation, given by:

$$T_{skin} = \frac{R_n - \lambda E - G}{\rho C_p C_h |U_a|} + T_a \tag{7}$$

where R_n is the net radiation (W m^{-2}), λE is the latent heat flux (W m^{-2}), G is the ground heat flux (W m^{-2}), ρ is the air density (Kg m^{-3}), C_p is the air heat capacity (J m^{-3} K^{-1}), C_h is the surface exchange coefficient for heat and moisture (dimensionless), U_a is the surface layer wind speed (m s^{-1}), and T_a is the near-surface air temperature (K). Equation (7) is the surface energy balance expression, with the sensible heat flux (H) term expanded such that the relationship can be expressed in terms of T_{skin}. As the skin is treated as an infinitesimally thin layer, and has no thermal inertia (heat capacity) of its own, the skin temperature may be very sensitive to forcing (especially radiation) errors. This expression has to be solved iteratively due to the implicit relationship, as some of the terms on the right hand side of the equation also contain skin temperature. The ground heat flux is governed by the diffusion equation for soil temperature (T):

$$C(\theta) \frac{\partial T}{\partial t} = \frac{\partial}{\partial z} \left(K_t(\theta) \frac{\partial T}{\partial z} \right) \tag{8}$$

where C is the volumetric heat capacity (J m^{-3} K^{-1}) and K_t is the thermal conductivity (W m^{-1} K^{-1}), and both are functions of θ; θ is fraction of unit soil volume occupied by water; and t and z are time (s) and the vertical distance (m) from the soil surface downward (i.e., the depth), respectively. The K_t relationship used in the LSM, as suggested by McCumber and Pielke (1981), has been used in many land surface models (e.g., Noilhan and Planton,

1989; Viterbo and Beljaars, 1995). However, Peters-Lidard et al. (1998) showed that this approach tends to overestimate (underestimate) K_t during wet (dry) periods, and the surface heat fluxes are sensitive to the treatment of thermal conductivity. In the LSM, K_t is capped at 1.9 W m^{-1} K^{-1}. Chen and Dudhia (2001) suggested that several thermal conductivity formulations are needed to arrive at the best approach.

Expanding equation (8) for the ith soil layer yields:

$$\Delta z_i C_i \frac{\partial T_i}{\partial t} = \left(K_t \frac{\partial T}{\partial z} \right)_{z_i+1} - \left(K_t \frac{\partial T}{\partial z} \right)_{z_i} \tag{9}$$

where Δz_i is the thickness (m) of the i-th soil layer. The prediction of T_i is performed using the fully implicit Crank-Nicholson scheme. In the top layer the last term in equation (9) represents the surface ground heat flux and is computed using the surface skin temperature. The gradient at the lower boundary, assumed to be 3 m below the ground surface, is computed from a specified constant boundary temperature and is taken as the mean annual near-surface air temperature.

In the off-line mode, we forced the LSM with seven weather variables collected at the hourly intervals, *viz.*, temperature, windspeed, precipitation, specific humidity, solar radiation, downwelling long wave radiation and the station pressure. Downwelling longwave radiation was not measured from SESM sites and we computed using the formulation given by Sridhar and Elliott (2002) that uses temperature and vapor pressure. Since station pressure data was not available, from the archives of National Climate Data Center, we downloaded the station pressure for the closest site, Brewster, which is 40 km from the study site. This single station hourly station pressure data were used all of the SESMs. The soil temperatures from 10 cm, 25 cm and 50 cm were needed as a state variable to initialize the top three layers and 100 cm soil temperature was used for the bottom layer initialization.

Growing Season Simulation

In this investigation, the LSM simulations were carried out for two growing seasons between March 2005 and October 2006, using the input fields of weather, vegetation and soil information from each plot. The model runs were made for hourly intervals and one simulation (14,640 time steps per plot) was run for each of the 11 plots, for a total of 11 simulations. While it is beneficial to look at the diurnal pattern of surface energy-balance components, it is however, important that quantification of soil moisture and evapotranspiration at an aggregated time scale aids in drawing conclusion on hydrometeorological responses to various treatment of plots. It was therefore *a priori* to aggregate surface fluxes and soil moisture at daily and monthly time steps. The vegetation variability based on the LAI measurements and the subsequent vegetation fraction derivation found to be quite distinct across the treatments and the plots. Since LAI data was available only at 5 of the 9 SESM stations, for the remaining four SESM stations, we used LAI from similar topographical locations. For instance, combinations include SESM 2 and 5; SESM 3 and 4, SESM 6 and 9 and SESM 7 and SESM 8. Independent measurements of LAI were available for Pulse High and Pulse Low plots.

Between the two growing seasons, it is possible to visualize the variations in vegetation fraction computed based on LAI measurements and equations 1 and 2 (Figure 2). SESM1/Grazed/Low showed a bimodal peak for each year during the two growing seasons, peaking once in June and again in September due to grazing and the vegetation fraction was quite high, close to 0.6. The reduced vegetation activity in 2006 was possibly due to decreased precipitation especially between May and June. SESM 2/Press Disturbance/High and SESM 5/Press Disturbance/High, as expected, had the lowest vegetation fraction of less than 0.1 that could be attributed to the disturbance introduced in the system at this high position. Similar pattern was observed at SESM 6/ Press Disturbance/Low and SESM 9/Press Disturbance/ Low as well. For two consecutive growing seasons SESM 3/Control/High and SESM 4/Control/High showed a peak of about 0.4 but notably in the second growing season, the dip in May/June was observed due to lack of precipitation at this high location which was less pronounced at SESM 7/Control/Low and SESM 8/Control/Low located in the low topographic position. It is worthwhile to note that while the amount of precipitation received at this high and low positions did not differ greatly, the available moisture for plant activity significantly differed, both seasonally and annually between these two systems

Results

Total Water budget quantification

Trends in precipitation (Figure 3a) and the response of soil moisture and evapotranspiration for the entire study period (March 05 to October 06) presented in Figure 3b. The climatic variation in precipitation and the resulting water balance components across different SESMs were not totally surprising but they implied many interesting facts. Firstly, the precipitation totals for this 20-month period was between 900 and 1000 mm across the plots. The low elevation sites, SESM1/Grazed/Low, SESM 7/Control/Low and SESM 8/Control/Low, showed high evapotranspiration totals of about 500-550 mm and the high elevation sites had evapotranspiration of about 300 mm or less. The difference of about 250 mm in the evapotranspiration totals over this relatively short period between high and low elevation plots, when precipitation was about the same, is significant. Pulse High and Pulse Low plots showed a similar trend in evapotranspiration and soil moisture as other high and low topographic plots. The results of this investigation also demonstrated that the soil moisture storage remained somewhat similar over this period, regardless of the treatment and topographic positions. Long term averages of root zone soil moisture of about 75 mm remained constant for all of the SESMs, but clearly the unaccounted effective precipitation at the high elevations were high. Over all, while the treatments have certainly modified the evapotranspiration totals, effective precipitation of about 40-50 % from low elevation sites and >60 % from high elevation sites were not accounted for in the system that would otherwise be either in the vadose column beneath the root zone soil layers and therefore contributing to the localized lateral flow to the surface streams and open water bodies in the interdunal valleys or diffused in the ground water system beneath the Sandhills. This longer term hydrologic analysis is certainly a key to addressing the prognostics of water budget over the sandhills and recharge estimation. When discretized over time and space, in a relatively shorter time scale, the energy fluxes and in particular, evapotranspiration can "switch" the land surface condition between the two states quite frequently either as an atmospheric moisture sink or a source for moisture in the growing season, especially during the spring-summertime thunderstorm periods in this High Plains region.

Energy-budget Computation

The time series plot showing the hourly results of net radiation and ground heat flux and latent and sensible heat fluxes as well as monthly fluxes are shown in Figure 4 (a-e). Typical summer day peak net radiation in the afternoon hours as simulated by the NOAH-LSM model at SESM 1(Grazed) reached up to 600 W/m^2. This is the total available energy, further split into ground, latent and sensible heat fluxes, through combinations of heat conduction and convection as well as water vapor evaporation or condensation processes. The model first assigned part of the net radiation to latent heat flux whose magnitude primarily was due to the vegetation fraction, land cover information and soil moisture. Admittedly a big portion of net radiation was utilized by evapotranspiration from the grass cover at SESM1/Grazed/Low in the growing season which was on the order of 200-300 W/m^2. However, a remarkable part this available energy was used up for sensible heat flux and finally the residual net radiation was allocated as ground heat flux which ranged between -100 and 250 W/m^2. Note that soil thermodynamics algorithm of the model uses this surface energy conceptualization to compute skin temperature and in the coupled mode, it is one of the important variables subsequently called by the atmospheric module of the model, apart from latent heat and sensible heat flux estimates.

Our validation of the modeled surface energy balance components was achieved firstly by comparing the hourly averages of simulation results with net radiation which was followed by ground heat flux at this high resolution (W/m^2). Over all, the model simulated net radiation very well seen from the scatter plot (Figure 4 a) and accurate prediction of net radiation was necessary because any discrepancy at this level of net radiation simulation would impact other estimates of energy-balance components later on. Secondly, two sets of ground heat flux measurements from 6 cm below the surface were averaged and compared with the model predicted ground heat flux closer to the surface. Predicted ground heat flux appeared reasonable for the sandy soils at this site that normally hold moisture content of about 10%. When comparing the estimated and observed ground heat flux one can see the higher estimates by the model and part of the reason for this problem was to do with discrepancy of the depths of comparison between the model estimates and measurements (Figure 4b). The observed ground heat flux variations were smaller than those of the model due to the neglect of the heat storage term above the 6 cm depth. Also, the ability of the model to compute the ground heat flux as the remainder of the energy budget often times led to assigning the residual as such which leads to overestimation. In other words, the model forced closure of the budget

8

at every time step by construct (i.e. force-restore method) and while there was no better alternative, it was ideal to accurately predict ground heat flux with this approach. The estimation of latent and sensible heat flux was not directly compared with measurements as it was not available at the time of this study. However, an attempt has been made to compare the water balance, especially soil moisture, by which model was validated for the other variables.

SESM 7/Control/Low plot was subjected to control treatment at the low topographic position. It exhibited two good growing seasons, based on the LAI/vegetation fraction information (Figure 2). Partitioning of the surface energy fluxes modeled at SESM 7/Control/Low showed some differences when compared with that of SESM 1/Grazed/Low. Perhaps, control treatment at SESM 7/Control/Low had resulted in a slightly higher vegetation fraction. But by closely looking at soil moisture that was available for the plant activity, it was revealed that even though SESM 7/Control/Low received the highest precipitation among all SESMs, the reduction in precipitation during March-May in the second growing season and grazing at SESM1/Grazed/Low could have resulted in higher soil moisture utilization and hence a marginally higher latent heat flux. Our analysis from SESM1/Grazed/Low showed that about 57 % of evapotranspiration to precipitation ratio in the first growing season (March-October 05) and 60% in the second season (March-October 06) in the grazed plot suggested that water consumption was slightly higher when the plot was grazed around July of each season when compared to the control plot values. As the precipitation decreases, evapotranspiration to precipitation ratio went up. In other words, the extraction efficiency was higher when grazed, especially when precipitation input was reduced due to natural climate variability. Whereas SESM 7/Control/Low the plot was subjected to control treatment and evapotranspiration to precipitation ratio was 50 and 53 % for first and second growing season, respectively. By comparing 57% and 60% of evapotranspiration to precipitation ratio to the control values of 50% and 53%, we can conclude that a considerable difference of 7% between the two growing seasons' water consumption was seen. From Figure 4e , it can be seen that reduced latent heat flux and more sensible and ground heat flux at the control plot, SESM 7/Control/Low and it suggested that even though the grass cover was active with good supply of soil moisture, transpiration by the plants was less by about 50 mm for the two seasons. Other SESM hourly simulation results for low sites (SESM 6, 8, and 9) indicated that net radiation was not distinctly different but latent heat flux was ranging between that of SESM1/Grazed/Low and SESM 7/Control/Low and approximately an equal distribution of sensible heat flux and latent heat flux was noticed.

Relevance of topography in the diurnal energy-balance

Figure 5 (a-e) shows the hourly simulation results of the surface energy balance for SESM 2/Press Disturbance/High that was subjected to press disturbance at the high location (vegetation fraction was less than 0.2). The importance of vegetation cover at this semi-arid region was significant from the latent and sensible heat flux estimates. While the model underestimated net radiation on the order of 100 W/m^2(Figure 5a), the uneven distribution of this energy between latent and sensible heat flux was evident. One possible explanation for the discrepancy in the predicted and observed net radiation is that the disturbance treatment and its strong relation to net radiation via albedo and evapotranspiration has not been well captured by the model and often times it is ignored in the model formulation. Disturbance causes dead biomass leading to an intermediate condition between vegetated and bare soil condition for some period of time. Hence parameterization of albedo for this surface condition remains a challenge and it plays a critical role in partitioning net radiation. On an average the growing season latent heat flux was only about 100 W/m^2 but not exceeding 200 W/m^2 for the entire season whereas sensible heat flux was as high as 400 W/m^2 for the same duration (Figure 5c). The magnitude of vegetation influence in differentiating the latent and sensible heat fluxes is evident as can be seen from Figure 5e, that it makes it important especially, when a condition without the native grass can be foreseen for the entire Sandhills which could be a trigger to mega droughts as we have seen in the past (Sridhar et al., 2006). Other SESM hourly simulation results are not shown here as the net radiation was not distinctly different but latent heat flux was low for the high SESMs (SESM 3, 4 and 5) and sensible heat flux was quite high. This was true for all control, press and pulse treatment plots. Quite surprisingly, the high topographic locations (SESM 2 and 3) had shown pronounced effect of this uneven partitioning of latent and sensible heat flux with latent heat flux being low. The Sandhills is interspersed with these high topographic locations or dunes and these results suggest that having an intact vegetation cover is important to maintain this ecosystem. However, the low topographic SESMs (SESM 7 and 8) not subjected to the same control treatment showed an equal partitioning between sensible and latent heat flux. Looking at the landscape scale, our results appeared to indicate that dunes with an elevation of 7 m or so in the Sandhills with less vegetation could potentially create an imbalance in the diurnal distribution of surface energy balance components, that is, net available energy is not equal to the sum of latent and sensible heat fluxes. The imbalance between net all-wave radiation and turbulent fluxes result from advection in these complex microtopographical variations. Also, net available energy when spent towards sensible

heat flux heating the soil and desiccating the soil moisture, it favors the persistence and continuation of the same conditions leading to higher sensible heat flux and lower latent heat flux. And the High Plains normally supplies moisture through evapotranspiration leading to convective precipitation events in the Spring and summer aided by Gulf of Mexico moisture flux. If this region dries out leading to lesser moisture supply to the atmosphere, it would only lead to increased drought conditions that can persist. Because splitting the net incoming energy into an enormous sensible heat flux and a decreased latent flux can persistently aggravate the heating and the desiccation of the land surface in a positive feedback scenario, it could further lead to a reversal of traditional "source" region for moisture during the summertime by turning it into a semi-arid desert.

Daily aggregated water and energy fluxes

The hourly simulation results were summed up to compute daily aggregated energy fluxes, accumulated ET and root zone soil moisture estimates. The results of daily net radiation, latent, sensible and ground heat fluxes for SESM 9/Press Disturbance/Low are shown in Figure 6. As a long-term or press disturbance plot at the low elevation, it was devegetated since August 2005. The interplay between vegetation and surface energy partitioning was abundantly clear from the simulated latent, sensible and ground heat fluxes and in particular between the high and low elevation sites. While the daily aggregated net radiation values were between 12-16 MJ/m^2/day which were reasonably high, a lesser latent heat flux due to less or no evapotranspiration and higher sensible and/or ground heat fluxes were seen as partitioned by the LSM model in the second growing season. Precipitation in the first and second growing season amounted to 443 mm and 428 mm, thus with a reduction of 15 mm. Similarly, the average air temperature between April and September for the first and second growing season showed some difference, 4.91 ºC and 4.85 ºC, respectively. However, relative humidity for these two years was 65% and 60%. Thus, the interannual variability for Press Disturbance plots showed some noticeable difference in precipitation, air temperature and relative humidity and this also collectively explained the lower evapotranspiration rates. Further analysis on soil moisture content provided insights into how the surface energy-budget and soil moisture were interconnected. Volumetric soil moisture (VWC) at 10, 25, 50 and 100 cm for SESM 9/Press disturbance/Low shown in Figure 7 indicates that the model captured well for all of the layers except the upper layer for two consecutive growing seasons. While the top three layers had relatively low soil moisture of 10%, the 100 cm layer had soil moisture between 10 and 25 % with an average of about 15%. Theta Probe measurements were made at a particular depth whereas the model simulated soil moisture represented the entire layer and it should be emphasized that in the absence of exactly matching soil depths observed soil moisture with that of the model the overestimation of model-simulated soil moisture as in Figure 6, especially for 100 cm can be partly explained. The Time-domain reflectometry (TDR) measurements however, showed good correlation with the model estimates as they represented the entire soil moisture layer as shown for the deeper layers, 30, 60 and 100 cms. The last panel in Figure 6 shows the computed root zone soil moisture, top 100 cm, simulated by the model (by summing soil moisture from 10, 30 and 60 cm layers) against observed root zone soil moisture (by summing soil moisture at 10, 25 and 50 cm depths). Clearly, the agreements on a daily time step were quite close and the high soil moisture content resulted from precipitation events was seen with periodical spikes in both observed and modeled root zone soil moisture. The range of average daily root zone soil moisture was between 60 and 120 mm, with an average of about 85 mm at this low elevation site.

The daily results of energy-budget partitioning for SESM1/Grazed/Low are not shown here but once again, the comparisons between simulated and observed net radiation showed a strong correlation. Barring the depth discrepancy, simulated ground heat flux also matched agreeably well with observed ground heat flux. While latent heat flux estimates were slightly higher from this plot, sensible heat flux was less as the soil was not barren and the vegetation cover had influenced this near surface process effectively. Vegetation that was present in this plot for the two consecutive growing seasons, and that presented an obvious and palpable scenario when combining energy fluxes and soil water content. The plant activity had generally lowered soil moisture and was predominantly between 5-10 % especially in the top three layers and this was low when compared to SESM 9/Press Disturbance/Low, even though both were located in the low topographic positions. Root zone soil moisture ranged between 20 and 120 mm. Depletion of soil moisture was clearly visible immediately by the end of the growing season in 2005 and matched particularly well between the model-simulated and the TDR-based soil moisture. Soil layers were once again recharged between January and March and the depletion was noticeable for the second growing season. What could have caused the difference in evapotranspiration and soil moisture behavior between SESM1/Grazed/Low and SESM 9/Press Disturbance/Low, even though both were located at the low topographic positions, on an aggregated daily time step? It was simply due to vegetation cover that played a significant role in root water extraction while

their diurnal maximum of latent and sensible heat fluxes were in the similar range, 200-300 W/m^2 and 300-400 W/m^2, respectively.

The analysis of daily energy-balance components and soil moisture distribution for SESM 5/Press Disturbance/High resulted in a higher sensible heat flux than latent heat flux because of lack of vegetation. And the daily time scale of net radiation and its split showed that combined sensible and ground heat flux was a much larger portion than latent heat flux alone. For a high topographic site such as SESM 5/Press Disturbance/High and other similar sites, while the soil moisture gradients in the upper three layers were only on the order of 3-10 %, the bottom 100 cm soil layer moisture was also only in the range of 7-15% with an average of 10% or less. This was also noticed with the TDR measurements at the same location and the reduced soil moisture at the deeper layers was not unusual at the dune tops. The overall reduction in the layer-wise moisture at the dune tops stretched the root zone soil moisture also to a reduced level of 60 mm, less by about 20 mm on average when compared with the low elevation sites. Once again, the results suggest that after the threshold vegetation cover was lost, regardless of the treatment and precipitation variability, the soil water distribution was predominantly driven by the topography that was quite distinct at the daily intervals, and the dune tops were vulnerable for rapid drying relative to the dry interdunal valleys. Therefore, it is easy to construe the combined effect of surface energy-balance at the sub-daily scale and soil moisture and or evapotranspiration at the daily scale can potentially distinguish how the dune tops and the interdunal valley could behave for the same vegetation and environmental conditions.

Seasonal estimates of ET and soil moisture

The hydrologic behavior analysis of any system at a given scale such as a plot, a watershed or an ecosystem over longer time scales is considered as appropriate for many reasons. Especially, tracking the movement of precipitation through surface and sub-surface processes including root zone soil water extraction by plants, deep percolation and recharge to groundwater have a time delay associated with them. Monthly analysis of evapotranspiration and soil moisture is a first step toward understanding how the treatment and vegetation played a role in response to climatic factors and how they differed in this two-year period. The comparisons could be made only with soil moisture and it is assumed that evapotranspiration estimates were reasonable, given the accuracy in estimating daily and monthly soil moisture, hourly and daily net radiation and ground heat flux as discussed in the previous section. Monthly aggregated soil moisture and evapotranspiration for low elevation SESMs, namely SESM 1/Grazed/Low, SESM 6/Press Disturbance/Low, SESM 7/Control/Low, SESM 8/Control/Low and SESM 9/Press Disturbance/Low are shown in Figure 8.

Monthly totals of evapotranspiration of SESM 1/Grazed/Low, SESM 7/Control/Low and SESM 8/Control/Low were close to 75 mm in June 2005 as this first growing season had good vegetation cover (Figure 2) and moisture supply and 50 mm in June 2006. Precipitation received for the month of June 2005 was 120 mm. It was the second highest monthly precipitation total after April 2005 which was about 123 mm. Evapotranspiration estimates from other SESMs were close to 50 mm for the same period due to senescence, all of the SESMs had reduced activity between September and March. The second growing season, however, resulted in reduced evapotranspiration as both observed and modeled root zone soil moisture were much less when compared with the previous growing season. Despite the grazing and control treatments, the behavior of all low SESMs, SESM 1(Grazed) and SESM 7 (Control) or SESM 8 (Control) were quite distinct interannually within themselves simply because of a monthly difference of about 25 mm or 50% variability in evapotranspiration from year to year.

Further investigation into the precipitation variability between SESM1/Grazed/Low and SESM 7/Control/Low revealed that these two had a different precipitation totals for the two years of study. SESM1/Grazed/Low had a precipitation of 500 and 425 mm of March through October for 2005 and 2006, respectively and SESM 7/Control/Low had 520 mm and 453 mm for the same period. A decrease of 15 % and 13 % in precipitation between March-October totals for 2005 and 2006 from SESM 1/Grazed/Low and SESM 7/Control/Low was noticed. While this difference was nominal from year to year, the time of precipitation mattered most in this case. For instance, March-April-May precipitation for SESM 1/Grazed/Low was 274 mm and 117 mm for 2005 and 2006, respectively and this 57% reduction in precipitation in the early growing season was nothing but extraordinary in reducing evapotranspiration and soil moisture in two consecutive years by about 33% while the vegetation condition did not vary significantly. Similarly, SESM 7/Control/Low had received the precipitation total of 290 mm between March-April-May in 2005 and 133 mm for the same period in 2006, thus having a reduction of 54 % in precipitation during the early growing season and a reduction of both evapotranspiration and soil moisture by about 33 %. It may be

surmised that irrespective of control or grazing treatment, year to year variability in precipitation especially in the early growing season, was found to have introduced large fluctuations in the monthly evapotranspiration totals and changes in soil moisture between SESM 1/Grazed/Low and SESM 7/Control/Low. Noticeably, SESM 6/Press Disturbance/Low and SESM 9/Press Disturbance/Low, had no vegetation and it helped to recharge the soil layers with moisture levels of up to 75-100 mm as monthly averages while the precipitation totals and distribution remained similar to that of SESM1/Grazed/Low. The treatment at these plots with the reduced vegetation activity resulted in the reduction of evapotranspiration by about 50 % between the two seasons. And the decrease in soil water content in the second year was quite proportionate to the reduced vegetation activity. Therefore, while vegetation treatment could be the dominant player for this reduced evapotranspiration, decreased precipitation could account for the reminder of year to year variance in evapotranspiration and soil moisture.. The results suggested that short term fluctuation (on a daily and sub-daily intervals) in the energy-balance partitioning was appreciable to some extent at the interdunal valley but daily and monthly trend in soil moisture and evapotranspiration partitioning can be significant, the fundamental drivers being vegetation and its treatment and precipitation.

Yet, soil moisture in the root zone from both SESM 6/Press Disturbance/Low and SESM 9/Press Disturbance/Low remained high and this increased soil moisture for the entire season in the sandy soil could be expected to add to recharge of the ground water system in the sandhills that has the porosity of about 35%, however, ground water level assessment at these plots would be of particular significance to ascertain categorically, if we were to close to the water budget more precisely and that is out of scope for this paper. Furthermore, even though the interdunal valley is mostly dry at the GDEX site, wet valleys and the appearance of ephemeral ponds between October and April are ubiquitous in the sandhills as observed by the authors. This also suggested that recharge zones at the low elevation sites existed but subsurface soil and flow characteristics including hydraulic conductivity, isotropy, lateral flow and water level data are necessary to draw conclusions in conjunction with the above-ground characteristics and moisture replenishment for the plant activity. Perhaps this will provide clues to address if in fact, surface desiccation combined with dry southwesterly winds alone would be a sufficient ingredient to activate the dunes of the Sandhills as it happened earlier (Sridhar et al., 2006) or the water table would also have to recede to a "hydrologic threshold" level which is essentially a level at which the surface energy-balance at the diurnal scale and water balance at the daily scale becoming independent of water table fluctuations beneath the dunes for a few consecutive growing seasons.

Figure 9 presents monthly water budget for high elevation sites, SESM 2/Press Disturbance/High, SESM 3/Control/High, SESM 4/Control/High and SESM 5/Press Disturbance/High . As again, variations in evapotranspiration estimates between press and control treatments were distinct. SESM 2/Press Disturbance/High and SESM 5/Press Disturbance/High showed little or no evapotranspiration since the vegetation was dead after August 2005 whereas SESM 3/Control/High and SESM 4/Control/High showed evapotranspiration of about 50 mm in June 2005 and 25 mm in June 2006. The 50% reduction in the monthly totals of evapotranspiration between the two consecutive growing seasons in the control setting was recognizable and similar explanation can be given that precipitation variability in the early growing season between 2005 and 2006 influenced these reductions. The uplands soil moisture storage in general, ranged between 50-75mm, which was similar to that of the low elevation sites shown in Figure 9 but interestingly the plant activity-induced soil moisture fluctuation was minimal for SESM 2/Press Disturbance/High and SESM 5/Press Disturbance/High in the first growing season and no drawdown at all in the second season for all of the upland SESM sites. In other words, precipitation variability did not bring about changes in the soil moisture conditions, and vegetation alone can significantly alter both short-term energy balance and long term water balance quite remarkably, more so at the dune tops. Monthly average of root zone soil moisture fluctuated only moderately in all of the high topographic locations, and the significant drawdown in soil moisture in July first growing season and in general, the long-term average of the root zone moisture was close to 50 mm which was relatively low.

So, except the magnitude, this phenomenon of root water extraction and soil water depletion at the root zone found to be similar in both low and high control and grazed SESM sites. And, if there was no vegetation activity, the soil layers tended to retain the moisture, which obviously could be directed to recharge over the long term and that can only be validated by concurrent measurements of water levels from the high soil moisture plots. While the soil water process is non-linear, the above findings presented a straightforward interpretation of the interactions between vegetation, soil moisture and evapotranspiration which is a simplified characterization of the complex exchange processes that is unique to the Sandhills.

Summary and conclusions

The use of high resolution spatio-temporal measurements of the vegetation activity, soil moisture states and weather variables combined with various treatment exercises provided a unique opportunity to quantify the variability as well as similarity in surface energy and water budgets at the GDEX site. With respect to the modeling effort, we demonstrated the applicability of NOAH Land Surface Model for various treatments and the success in simulating both high and low topographic plots quite distinctly. Specific conclusions of this investigation include:

- Despite similarities in the forcing and soil conditions, merely dune topography, and the vegetation condition on the dune tops can significantly alter the partitioning of water budget in this sandhills ecosystem. This is especially true when the long term totals of evapotranspiration between high and low plots differed up to about 250 mm in a relatively short 20-month period comprising two growing seasons.
- Even though the amount of precipitation received was between 900 and 1000 mm in total, on a daily and sub-daily time scale, we showed how non-linear the system can be while partitioning net radiation that was available for latent, sensible and ground heat fluxes. Monthly totals of evapotranspiration and soil moisture averages demonstrated the influence of amount and timing of precipitation in modulating evapotranspiration between the two consecutive growing seasons.
- However, there are some issues upon us to resolve in order to exactly partition and close the water budget at a longer time scale and to trace the fate of effective precipitation in the sub-surface system and accounting them as recharge or lateral flow in the three-dimensional array of surface, sub-surface and atmospheric systems over space and time.
- In the context of land and water resource management, this investigation pointed out the importance of vegetation over the sandhills and it will form the basis for understanding how they can be relevant to the resilience of the ecosystem. This study highlighted the necessity for closely monitoring this largest managed ecosystem, the Sandhills, given the fact that positive land-atmospheric feedback in a dry year could trigger prolonged drought when combined with larger westward shift in the modern day wind regimes causing potential destabilization of dunes in the region.

References

Chen F, Dudhia J. 2001. Coupling an advanced land-surface/hydrology model with the Penn State-NCAR MM5 modeling system. Part I: Model implementation and sensitivity. *Monthly Weather Review* **129**: 569-585.

Chen X, Hu Q. 2004. Groundwater influence on soil moisture and surface evaporation. *Journal of Hydrology* **297**: 285-300.

Cuenca RH, Ek M, and Mahrt L. 1996. Impact of soil water property parameterization on atmospheric boundary-layer simulation. *Journal of Geophysical Research* **101**, 7269-7277.

Dirmeyer PA. 1994. Vegetation stress a feedback mechanism in midlatitude drought. *Journal of Climate* 1463-1483.

Eberbach PL. 2003. The eco-hydrology of partly cleared, native ecosystems in southern Australia: a review. *Plant and Soil* **257**: 357-369.

Ek M, Mahrt L. 1991. OSU 1-D PBL model user's guide. Department of Atmospheric Sciences, Oregon State University, Corvallis, Oregon 97331-2209.

Entekhabi D, Rodriguez-Iturbe I, Bras RL. 1992. Variability in large-scale water balance with land surface-atmosphere interaction. *Journal of Climate* **5**: 798-813.

Gutman G, Ignatov A. 1998. The derivation of the green vegetation fraction from NOAA/AVHRR data for use in numerical weather models, *Intl.J. Remote Sens.*, 19, 1533-1543.

Hanks RJ, Aschcroft GL. 1986. *Applied Soil Physics.* Springer-Verlag, NY, 159pp.

Jackson TJ, Le Vine DM, Hsu AY, Oldak A, Starks PJ, Swift CT, Isham J, Haken M. 1999. Soil moisture mapping at regional scales using microwave radiometry: the Southern Great Plains Hydrology Experiment. *IEEE Transactions on Geoscience and Remote Sensing*. **37**: Issue 5, Part 1, pp. 2136-2151.

Jacquemin B, Noilhan J. 1990. Sensitivity study and validation of a land surface parameterization using the HAPEX-MOBILHY dataset, *Boundary-Layer Meteorology* **52**: 93-134.

Kahan DS, Xue Y, Allen SJ. 2006. The impact of vegetation and soil parameters in simulations of surface energy and water balance in the semi-arid sahel: A case study using SEBEX and HAPEX-Sahel data. *Journal of Hydrology* **320**: 238-259.

Lakshmi V, Wood EF. 1998. Diurnal cycles of evaporation using a two-layer hydrological model. *Journal of Hydrology* **204**: Issue 1-4, pp. 37-51.

Li J, Islam S. 2002. Estimation of root zone soil moisture and surface fluxes partitioning using near surface soil moisture measurements. *Journal of Hydrology* **259**: Issue 1-4, pp. 1-14.

Mahrt L, Ek K. 1984. The influence of atmospheric stability on potential evaporation. *Journal of Climatology and Applied Meteorology* **23**: 222-234.

McCumber MC, Pielke RA. 1981. Simulation of the effects of surface fluxes of heat and moisture in a mesoscale numerical model soil layer. *Journal of Geophysical Research* **86**: 9929-9938.

Mohanty BP, Famiglietti JS, Skaggs TH. 2000. Evolution of soil moisture spatial structure in a mixed vegetation pixel during the Southern Great Plains 1997 (SGP97) Hydrology Experiment. *Water Resources Research* **36**: Issue 12, pp. 3675-3686.

Murphy RE. 1992. First ISLSCP field experiment (FIFE). *Journal of Geophysical Research* **97**: Issue D17, pp. 18,343-19,109.

Nicholson S. 2000. Land surface processes and sahel climate. *Review of Geophysics* **38**: 1, 117-139.

Noilhan J, Planton S. 1989. A simple parameterization of land surface processes for meteorological models. *Monthly Weather Review* **117**: 536-549.

Peters-Lidard CD, Blackburn E, Liang X, Wood EF. 1998. The effect of soil thermal conductivity parameterization on surface energy fluxes and temperatures. *Journal of Atmospheric Science* **55**: 1209-1224.

Sandvig RM, Phillips FM. 2006. Ecohydrological control on soil moisture fluxes in arid to semiarid vadose zones. Water Resources Research **42**: W08422, doi:10.1029/2005WR004644.

Schaake JC, Koren VI, Duan QY, Mitchell K, Chen F. 1996. A simple water balance model (SWB) for estimating runoff at different spatial and temporal scales. *Journal of Geophysical Research* **101**: 7461-7475.

Sridhar V. 2007. Evapotranspiration estimation and scaling effects over the Nebraska Sand Hills. *Great Plains Research* **17**: 35-45.

Sridhar V, Elliott RL. 2002. On the development of a simple downwelling longwave radiation scheme. *Agricultural and Forest Meteorology* **112**: No. 3-4, 237-243.

Sridhar V, Loope DB, Mason JA, Swinehart JB, Oglesby RJ, Rowe CM. 2006. Large Wind Shift on the Great Plains During the Medieval Warm Period. *Science* **313**: No. 5785, pp. 345 – 347, DOI: 10.1126/science.1128941.

Sridhar V, Elliott RL, Chen F. 2003. Scaling effects on modeled surface energy balance components using the Noah Land Surface Model. *Journal of Hydrology* **280**: No. 1-4, 105-123.

Sridhar V, Elliott RL, Chen F, Brotzge JA. 2002. Validation of the NOAH-OSU Land Surface Model using surface flux measurements in Oklahoma. *Journal of Geophysical Research* **107**: No. D20, 4418, doi: 10.1029/2001JD001306.

Viterbo P, Beljaars AC. 1995. An improved land surface parameterization scheme in the ECMWF model and its validation. *Journal of Climate* **8**: 2716-2748.

Webb RH, Leake SA. 2006. Ground-water surface-water interactions and long-term change in riverine riparian vegetation in the southwestern United States. *Journal of Hydrology* **320**: 302-323.

Yunhao C, Xiaobing L, Xia L, Peijun S. 2003. Fractional vegetation cover estimation based on satellite-sensed land classification. Multispectral and Hyperspectral Remote Sensing Instruments and Applications, *Proceedings of SPIE* **4897**: 403-410.

List of Figure Captions

Figure 1. Location map of the study area. Note: BBR N5-N8 stands for Barta Brother Ranch Four Quandrants from NW, NE, SW and SW as N5, N6, N7 and N8. The figure shows Surface Energy balance and Soil Moisture (SESM) locations, LAI sampling points, and erosion end points.

Figure 2. Vegetation Fraction computed using leaf area index (LAI) for different treatments plots during Mar 05 - Oct 06.

Figure 3. (a) Precipitation analysis for five SESM stations during the study period. (b) SESM/treatment/topography based observed precipitation, modeled evapotranspiration, observed and modeled soil moisture

Figure 4. For the SESM 1/Grazed/Low plot (a) Hourly Observed and modeled net radiation showing good agreement with 1:1 line (b) Hourly Observed and modeled ground heat flux showing a bias towards the model (c-d) Time series plot of latent and sensible heat flux predicted by the model (e) Monthly surface energy balance components (net radiation, latent, sensible and ground heat fluxes) predicted by the model and comparisons with observed net radiation and ground heat flux

Figure 5. For the SESM 2/Press Disturbance/High plot (a) Hourly Observed and modeled net radiation showing good agreement with 1:1 line (b) Hourly Observed and modeled ground heat flux showing a bias towards the model (c-d) Time series plot of latent and sensible heat flux predicted by the model (e) Monthly surface energy balance components

(net radiation, latent, sensible and ground heat fluxes) predicted by the model and comparisons with observed net radiation and ground heat flux

Figure 6. Daily Energy balance components, net radiation, latent, sensible and ground heat fluxes for the SESM 9/Disturbance/Low plot predicted by the model is compared against observed net radiation and ground heat flux

Figure 7. Predicted and observed volumetric soil moisture for the SESM 9/Disturbance/Low plot at 10, 30, 60 cm and Root Zone Soil moisture (model at 100 cm vs. obs at 85 cm)

Figure 8. Monthly average observed and predicted soil moisture for the Low sites, SESM 1, 6, 7, 8 and 9 and predicted evapotranspiration

Figure 9. Monthly average observed and predicted soil moisture for the High sites, SESM 2, 3, 4 and 5 and predicted evapotranspiration

List of Table Captions

Table 1. Summary of Site Topographic Location, Plot Treatments and Climate

Table 1. Summary of Site Topographic Location, Plot Treatments and Climate

Surface-Energy balance and Soil Moisture (SESM) Sites	Topographic Location	Elevation (m)	Treatment	Weather Station	Mean Annual Temp. FY 2005 (°C)	Annual Total Precipitation FY2005 (mm)
SESM 1	Low	765.0	Grazed	All but P*	11.40	493.12
SESM 2	High	767.5	Press Disturbance	All[§]	11.74	515.50
SESM 3	High	767.3	Control	All[§]	12.17	492.80
SESM 4	High	769.2	Control	All[§]	11.76	519.00
SESM 5	High	768.8	Press Disturbance	All[§]	11.35	406.30
SESM 6	Low	766.5	Press Disturbance	All but P*	13.78	493.12
SESM 7	Low	763.1	Control	All[§]	11.79	532.00
SESM 8	Low	762.2	Control	All but P*	12.62	493.12
SESM 9	Low	763.4	Press Disturbance	All but P*	12.39	493.12
----------	High	-----	Pulse Disturbance	Avg. of SESM2,3,4 &5	11.83	502.40
----------	Low	-----	Pulse Disturbance	Avg. of SESM 1,6,7,8 & 9	11.50	525.10

Note: In the Weather station column, All but P* denotes the use of all weather variables at the respective SESM weather station except precipitation. Precipitation for these sites are the averages of SESM 2(PRESS DISTURBANCE), 3, 4, 5 and 7 collected from tipping bucket rain gages. Also, All[§] indicates precipitation, temperature, wind speed, solar radiation. Longwave downwelling radiation and specific humidity were derived for SESM 1 through SESM 9 (PRESS DISTURBANCE).
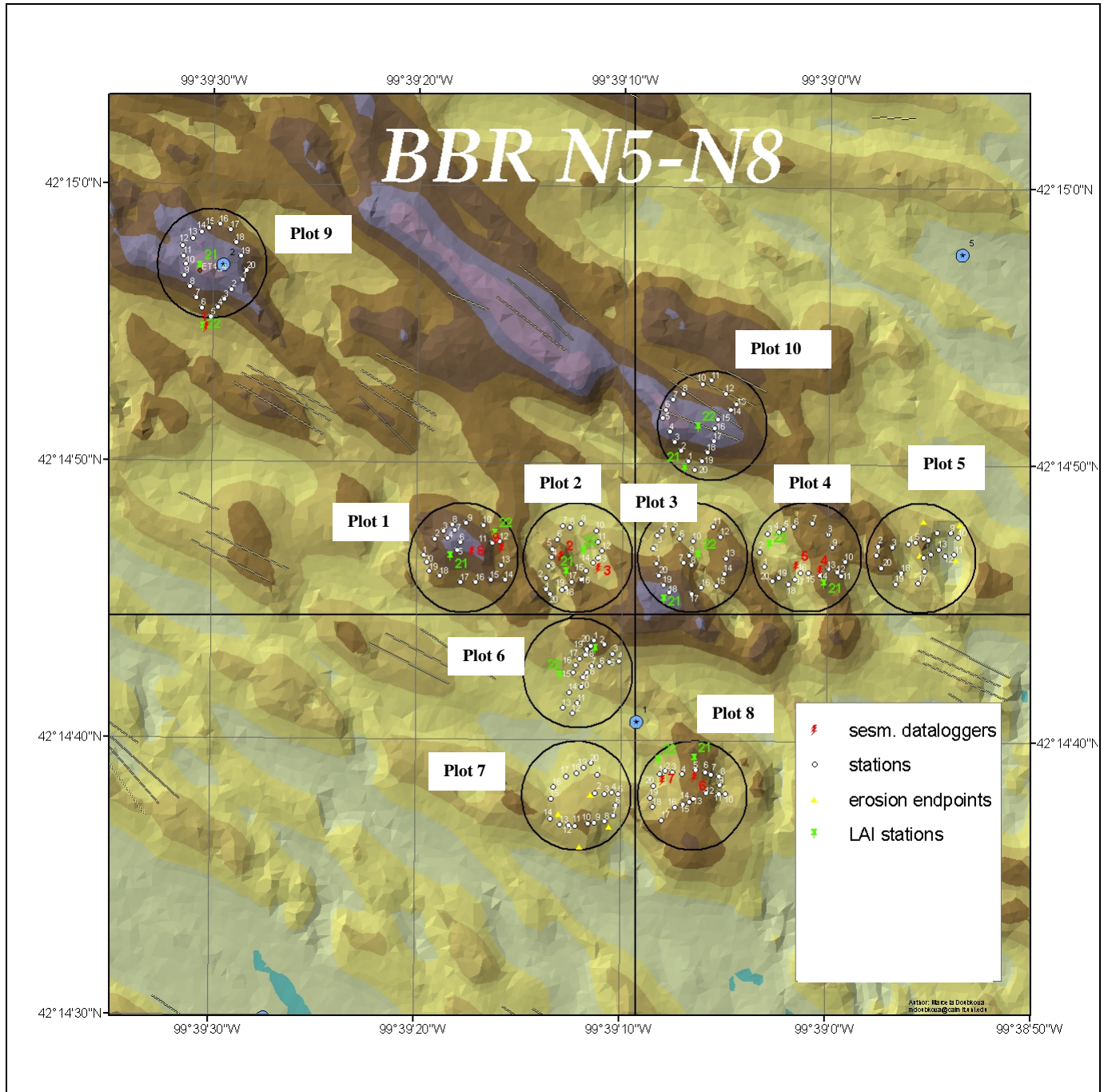
Figure 1
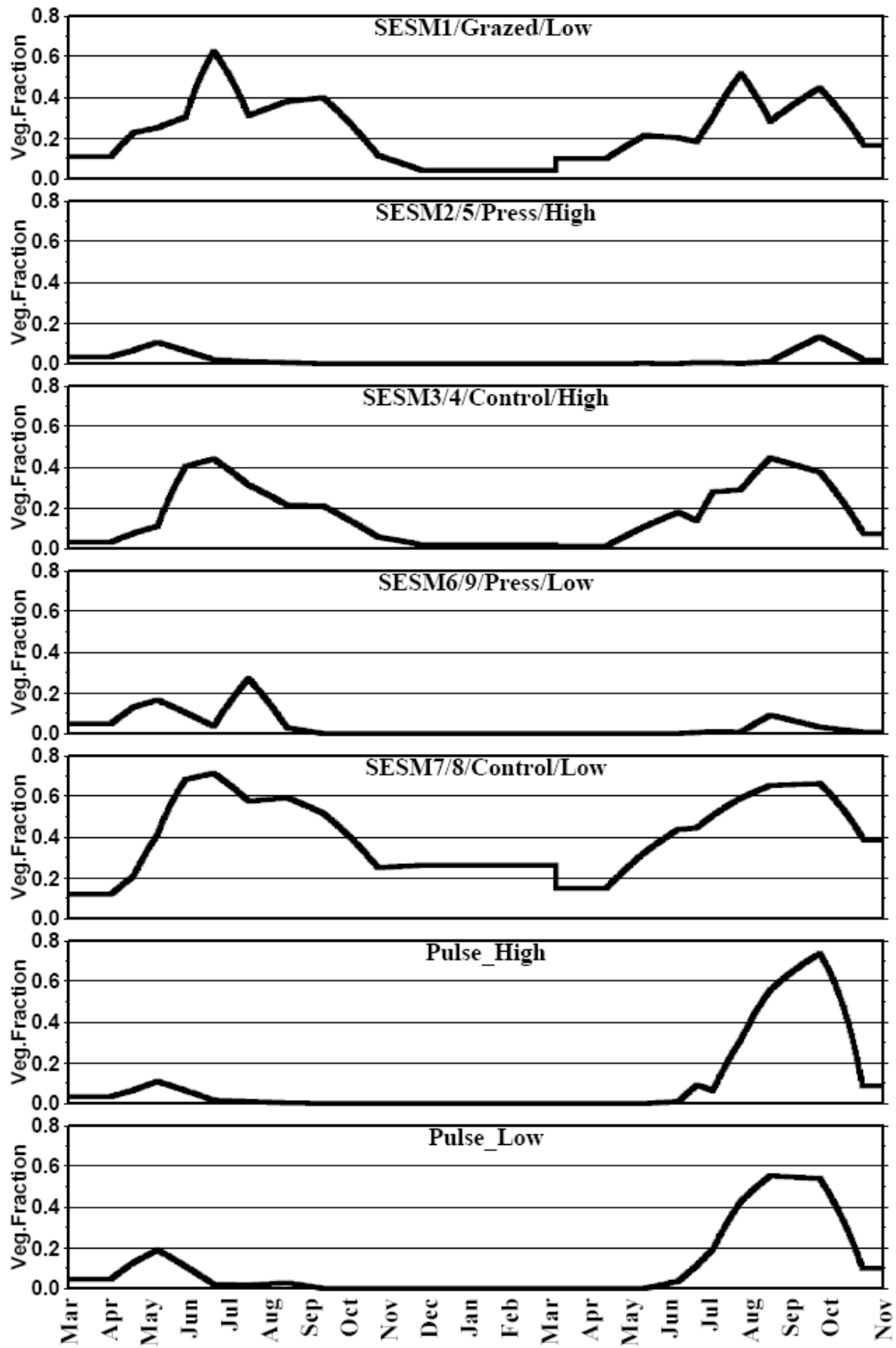
Figure 2
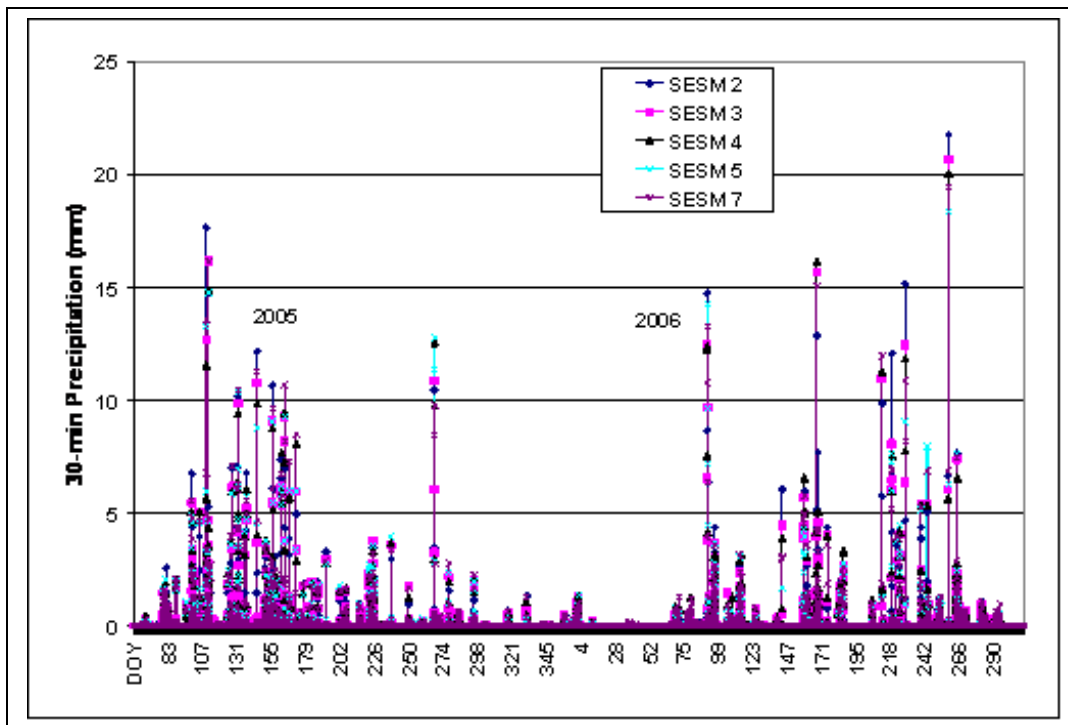
Figure 3 a
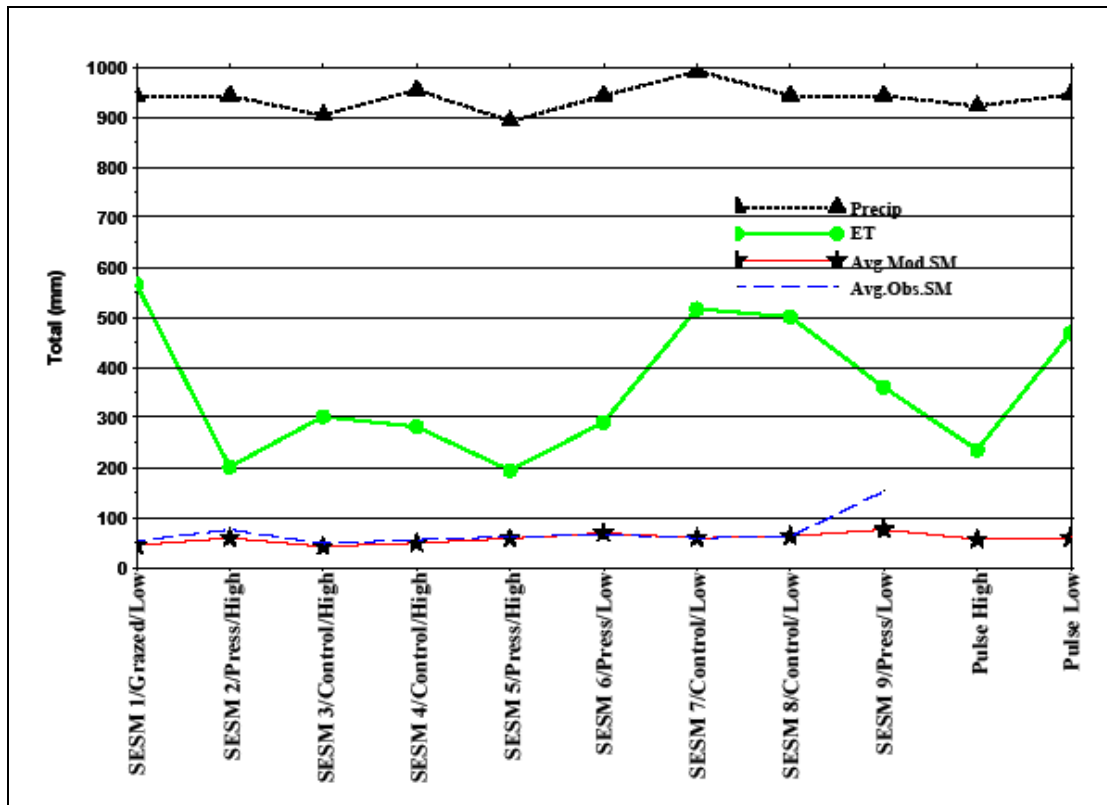
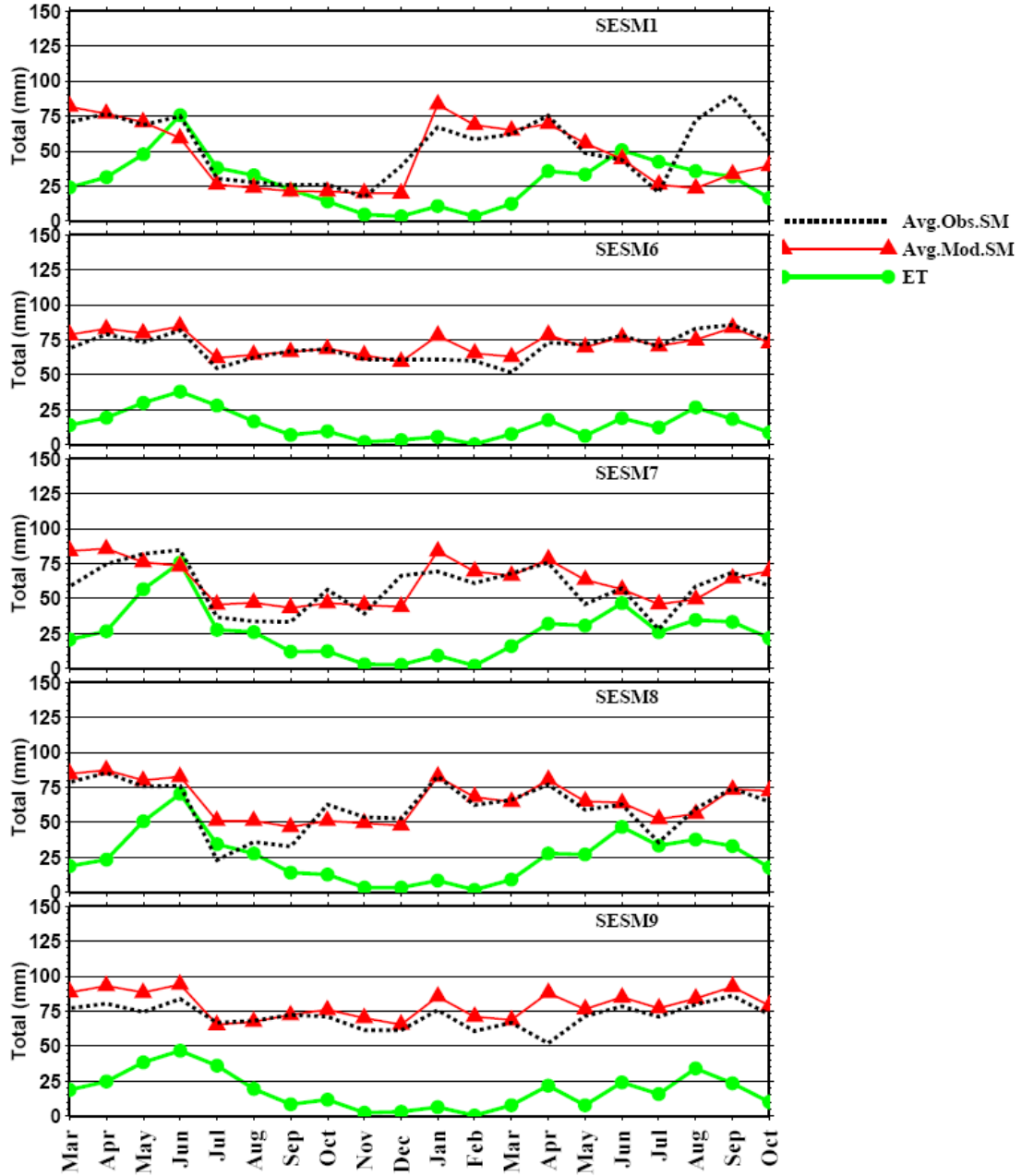Figure 3 b
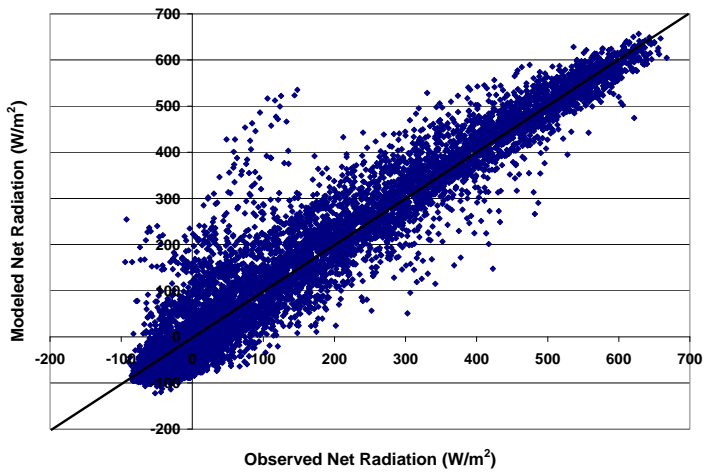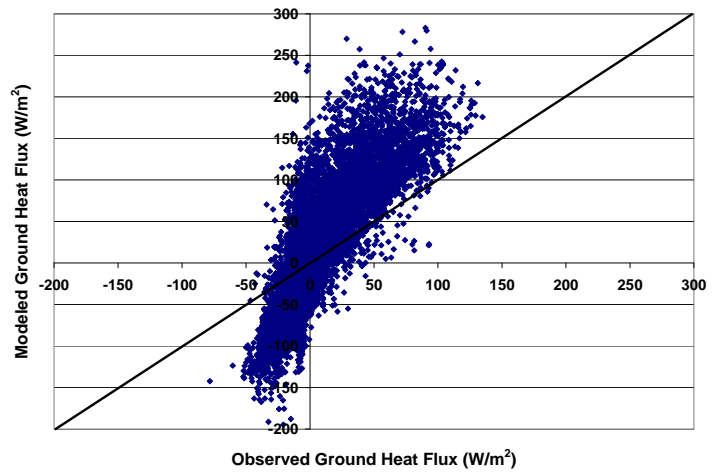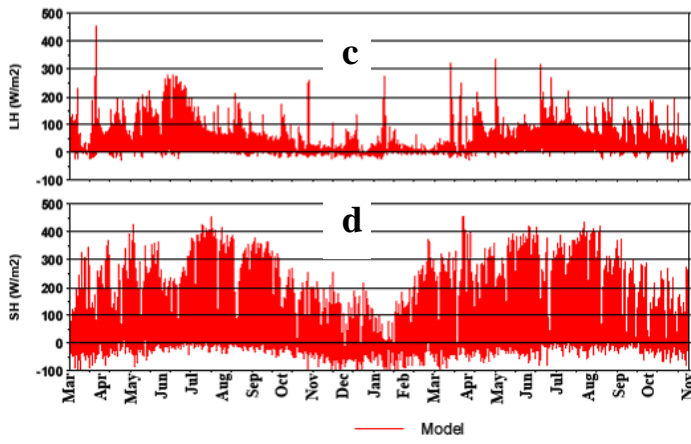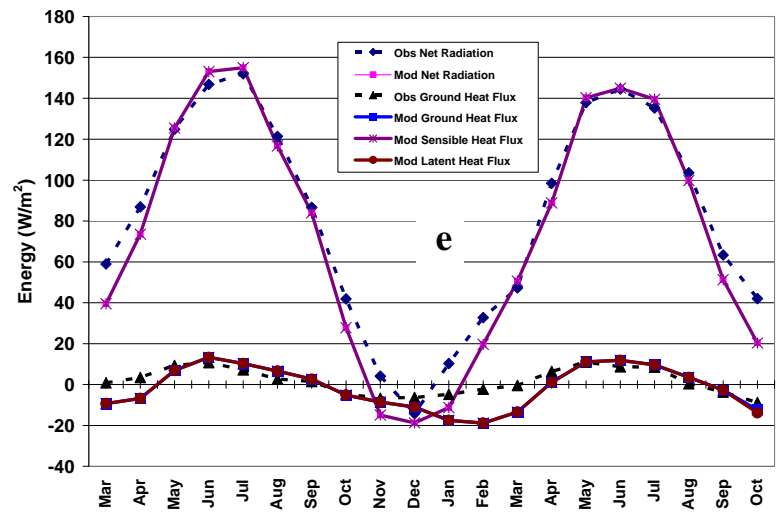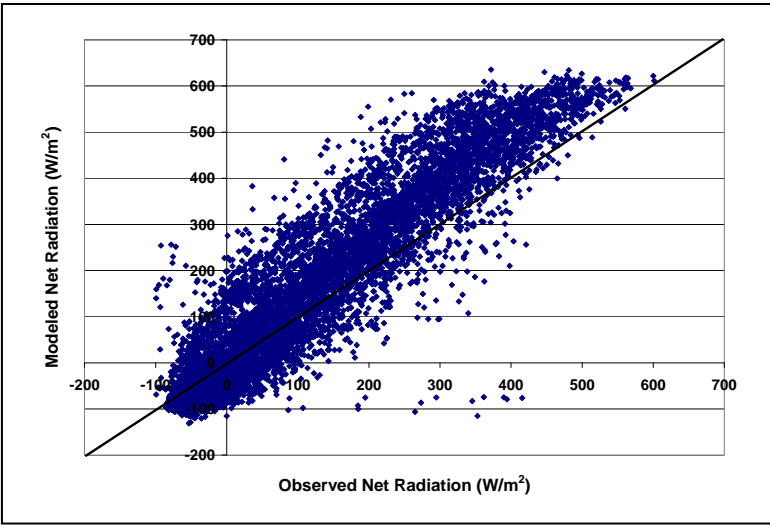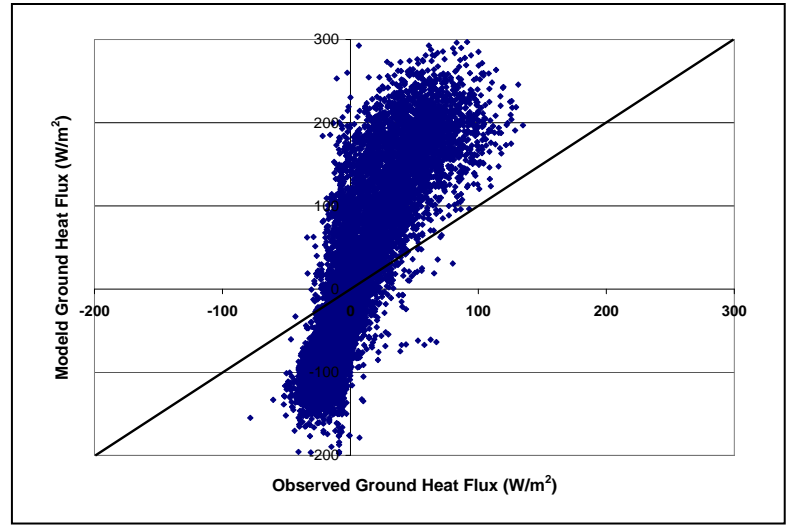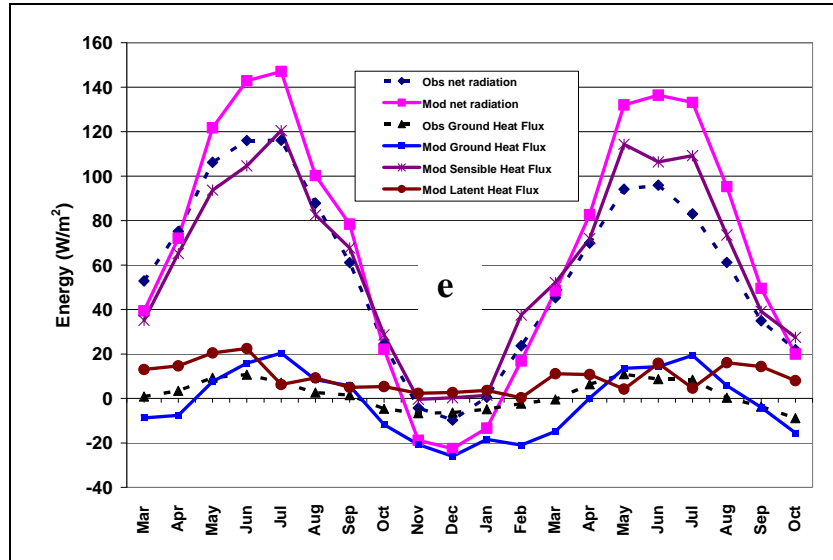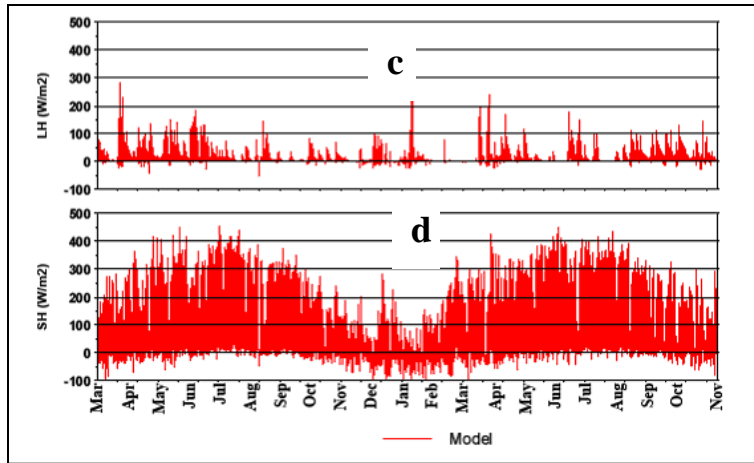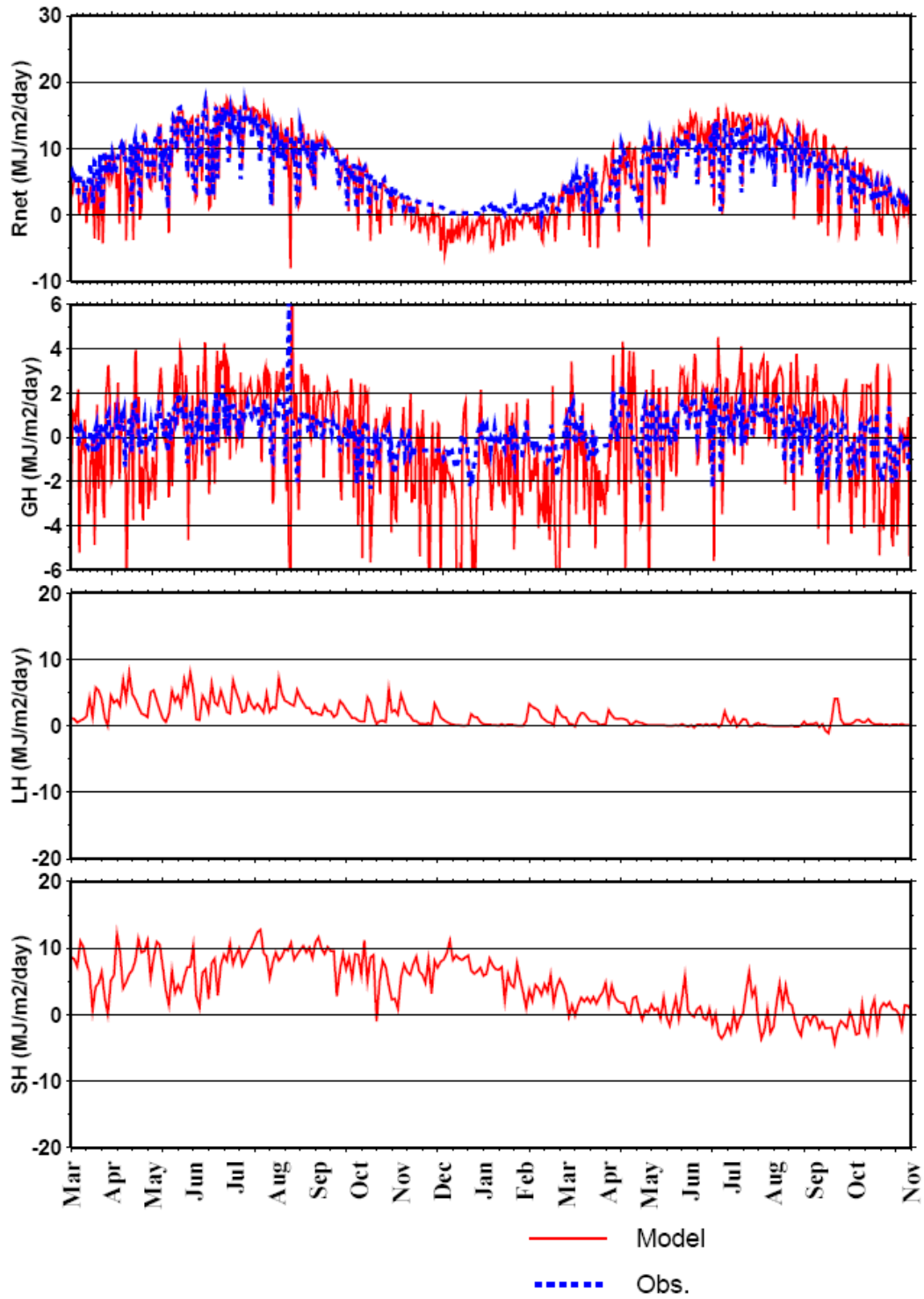
Figure 4

a

b

c

d

e

Figure 5

24

Figure 6

Figure 7

26

Figure 8

27
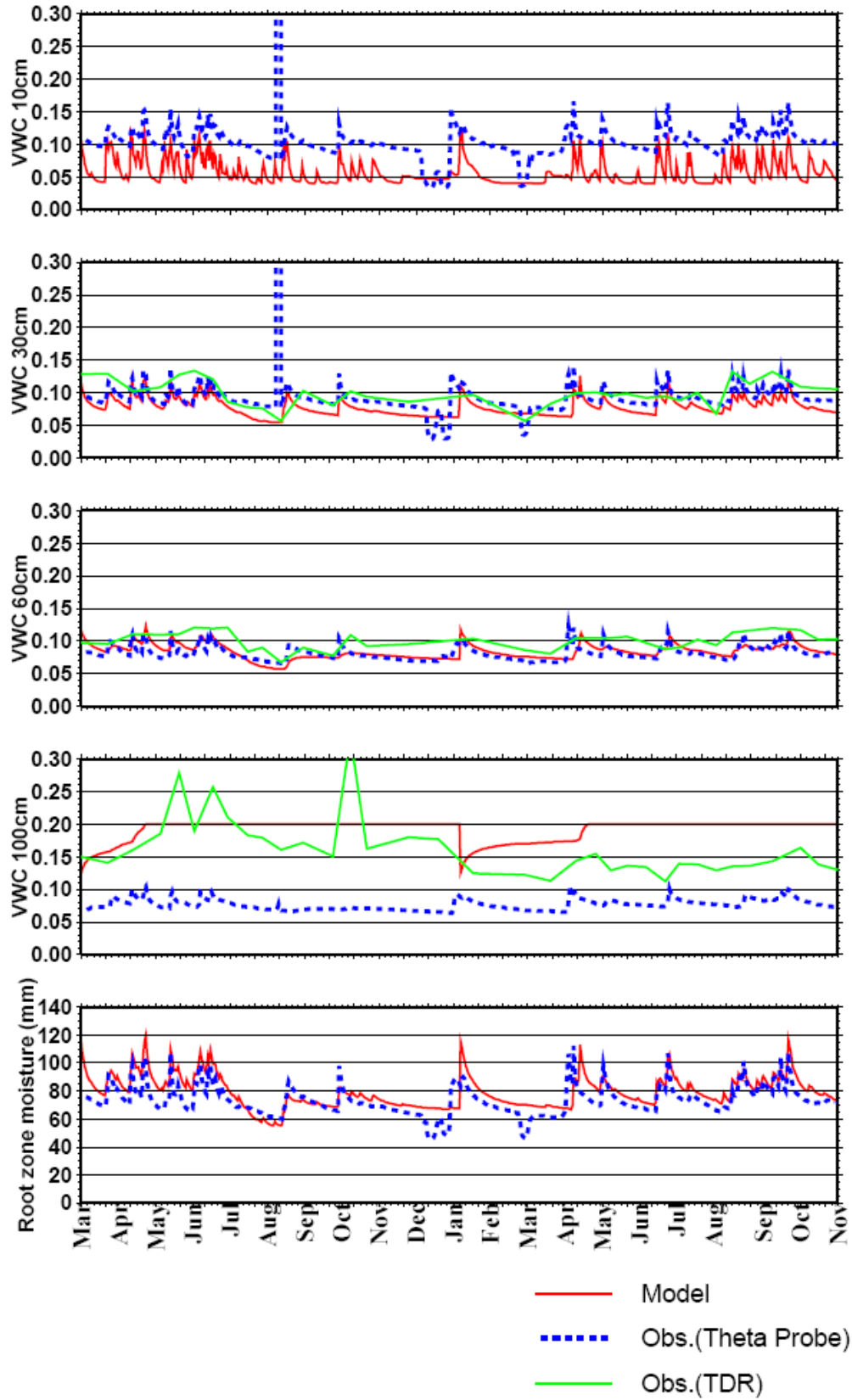
Hydrolgic Budget (Mar05-Oct06)

Figure 9